

Photoionization from metastable $(1s2s) \ ^1S^e$ and $\ ^3S^e$ states of the He atom for energies between the $N = 2$ and 3 thresholds of He^+

Bin Zhou and C. D. Lin

Department of Physics, Kansas State University, Manhattan, Kansas 66506

(Received 12 July 1993)

Photoionization cross sections from the metastable state $(1s2s) \ ^1S^e$ of the He atom for photon energies between the He^+ ($N = 2$) and ($N = 3$) thresholds are calculated using the hyperspherical close-coupling method. The calculated spectra are convoluted with an energy resolution of 5.4 meV and are compared with the spectra for photoionization from the ground state. It is found that among the four possible outgoing channels, the $1sep$ channel, which is the dominant channel for photoionization from the ground state, makes negligible contributions to the total cross sections for photoionization from the metastable state. As a result, the propensity rule derived from the ground-state photoionization no longer applies and more series of the doubly excited states are populated with significant spectral intensity in photoionization from the metastable state. Photoionization cross sections from the metastable $(1s2s) \ ^3S^e$ state are also calculated and analyzed.

PACS number(s): 32.80.Fb, 32.70.Cs, 31.50.+w, 32.80.Dz

I. INTRODUCTION

In an earlier paper [1], we have presented a calculation of photoionization of He from the metastable states $(1s2s) \ ^1S^e$ and $\ ^3S^e$, in the energy range below the He^+ ($N = 2$) threshold. It was found that the narrow doubly excited states with the approximate quantum number $A = -, 0$, which are weakly populated in photoabsorption from the ground state, are drastically enhanced in the photoionization spectra from the metastable states. This enhancement of $A = -, 0$ resonances was interpreted by the fact that doubly excited states associated with the $N = 2$ manifold consist mainly of the $2snp$ configuration [with exception for the $\ ^3P^o(A = 0)$ series which have about 30% of sp configurations, see [2]], therefore transitions from the initial state $(1s2s)$ to these states can be regarded essentially as the strong single-electron transition $1s \rightarrow np$. To examine the role of electron correlations in the photoionization process from the metastable states, it is more interesting to see the photoionization spectra for photon energies above the He^+ ($N = 2$) threshold where doubly excited states associated with the $N = 3$ manifold can be populated during which orbitals of *both* electrons have to be changed in the photoabsorption process. Also there is more than one outgoing channel to the continuum above the $N = 2$ threshold. It is the aim of this paper to extend the previous study on photoionization of He in the metastable states to the energy region between the He^+ ($N = 2$) and ($N = 3$) thresholds and to compare the spectra with the corresponding spectra from the ground state.

Very recently Sánchez and Martin [3,4] have calculated the spectra in the same energy range using the configuration-interaction method in conjunction with the Feshbach-O'Malley formalism and both the total and partial photoionization spectra were obtained. Here we will present our calculated spectra, which are in reasonably good agreement with their results. Here, however,

we shall emphasize comparison of the calculated spectra obtained for photoabsorption from the ground state and from the metastable states. In particular it is of great interest to check the validity of the propensity rule, which has been applied with great success to photoabsorption of He and He-like atomic systems in the ground state. The propensity rule predicts that only the $A = +$ series with the maximum K quantum number is primarily populated in the photoabsorption. However, we will show that this rule no longer works for photoionization from the metastable states where other series are also significantly populated.

It should be noted that although experimental works on photoionization of the He atom so far have been limited to He in the ground state, measurements from these metastable states should become possible in the near future, considering the increasing densities of the metastable atoms which can be produced today. Our results serve to guide experimentalists and their results are to be used to check against the theoretical predictions given in this paper.

In the next section, a brief description of the theoretical method used for the calculation is given. The results from both the $(1s2s) \ ^1S^e$ and the $(1s2s) \ ^3S^e$ states are presented and analyzed in Sec. III. A brief summary is given in Sec. IV.

II. THEORETICAL METHOD

The hyperspherical close-coupling method (HSCC) used in this work has been described in detail elsewhere [5,6]. Here we only give a brief review. Atomic units will be used throughout unless stated otherwise. As before, doubly excited states will be designated by $\ _N(K, T)_n^A$ or its simplified version K_n^A .

In the hyperspherical coordinates, with the two-electron wave function of He expressed by $\psi(\mathbf{r}_1, \mathbf{r}_2) =$

$\Psi(R, \alpha, \Omega)/(R^{5/2} \sin \alpha \cos \alpha)$, the Schrödinger equation can be written as

$$\left(-\frac{1}{2} \frac{\partial^2}{\partial R^2} + \frac{H_{\text{ad}}}{R^2} - E\right) \Psi(R, \alpha, \Omega) = 0, \quad (1)$$

where $R = \sqrt{r_1^2 + r_2^2}$ is the hyperradius, $\alpha = \tan^{-1} \left(\frac{r_1}{r_2}\right)$ is the hyperangle, and Ω denotes collectively four angles $(\hat{\mathbf{r}}_1, \hat{\mathbf{r}}_2)$. H_{ad} is the adiabatical Hamiltonian.

To solve the Schrödinger equation in the HSCC method, the configuration space is divided into two regions: an inner one ($R < R_M$) where the electron-electron interaction is strong and an outer or asymptotic region ($R > R_M$) where one electron is far away from the other and the electron-electron interaction is relatively weak.

In the inner region, the range of the hyperradius has been partitioned into many small sectors $[R_0, R_1, \dots, R_M]$. For a given sector, $R \in [R_{i-1}, R_i]$, $\Psi(R, \alpha, \Omega)$ is expressed in a close-coupling expansion

$$\Psi(R, \alpha, \Omega) = \sum_{\mu=1}^{N_{\text{ch}}} F_{\mu}(R) \phi_{\mu}(R_i^m; \alpha, \Omega) \quad (R_{i-1} < R < R_i), \quad (2)$$

where R_i^m is chosen to be at the midpoint of the i th sector, and N_{ch} channels are included. Note that channel functions ϕ_{μ} are *independent* of R within the sector.

Substituting (2) into the Schrödinger equation (1), one obtains the close-coupling equations for F_{μ} ,

$$\left(-\frac{\partial^2}{\partial R^2} - 2E\right) F_{\mu}(R) + \sum_{\nu} V_{\mu\nu}(R) F_{\nu}(R) = 0 \quad (\mu = 1, \dots, N_{\text{ch}}) \quad (3)$$

where the coupling term $V_{\mu\nu}(R)$ between the channels μ and ν is simply given by

$$V_{\mu\nu}(R) = \frac{2}{R^2} \langle \phi_{\mu}(R_i^m; \alpha, \Omega) | H_{\text{ad}}(R, \alpha, \Omega) | \phi_{\nu}(R_i^m; \alpha, \Omega) \rangle \quad (R_{i-1} < R < R_i). \quad (4)$$

By making the channel functions ϕ_{μ} independent of R in (2) within each hyperradial sector, often referred to as the diabatic-by-sector technique, the calculation of couplings $V_{\mu\nu}(R)$ among different channels is significantly simplified as one now can avoid direct computations of the derivatives of the channel function ϕ_{μ} with respect to R , which are difficult to handle numerically.

The calculation in the inner region proceeds in the following steps. First the diabatic channel functions ϕ_{μ} , thereby the channel couplings $V_{\mu\nu}(R)$ are calculated for each sector. Then starting from the innermost sector $i = 1$, the close-coupling equations (3) are integrated from R_{i-1} to R_i to obtain the radial functions $F_{\mu}(R)$, whose values at the end point R_i will serve as the initial boundary condition for the integration in the next sector. The integration propagates from inner sectors to outer ones, until the matching boundary $R = R_M$ is reached. The step size between any two adjacent sectors i and $(i + 1)$ is chosen to be small enough to ensure the

unitarity of the local transformation matrix

$$T_{\mu\nu}(i \rightarrow i + 1) = \langle \phi_{\mu}(R_i^m) | \phi_{\nu}(R_{i+1}^m) \rangle. \quad (5)$$

Beyond $R = R_M$, the two electrons are well separated and are described more adequately as products of two hydrogenic functions in the independent electron coordinates r_1, r_2 ,

$$\psi_E^{(\beta)}(\mathbf{r}_1, \mathbf{r}_2) = \frac{1}{r_{<} r_{>}} \sum_{i=1}^{N_{\text{r}m\text{ch}}} \Phi_i(r_{<}) Y_{l_1 l_2}^{LM}(\Omega) \times [f_i^E(r_{>}) \delta_{i\beta} - g_i^E(r_{>}) K_{i\beta}(E)] \quad (\beta = 1, \dots, N_{\text{ch}}), \quad (6)$$

where $r_{<} = \min(r_1, r_2)$ and $r_{>} = \max(r_1, r_2)$. Φ_i is the bound hydrogenic radial function of nuclear charge $Z = 2$ of the inner electron for channel i characterized by the binding energy $E_i = -\frac{2}{N(i)^2}$ with $N(i)$ as the inner electron's principal quantum number. $Y_{l_1 l_2}^{LM}(\Omega)$ is the coupled spherical harmonic function formed by angular momentum l_1, l_2 of the two electrons. The functions f_i, g_i are the energy-normalized regular and irregular radial Coulomb functions of charge 1, respectively, of the outer electron if channel i is open ($E \geq E_i$), or exponentially increasing and decreasing functions if i is closed ($E < E_i$).

Similar to the R -matrix method, the reaction matrix \mathbf{K} is obtained when the numerical solution and its derivative with respect to R in the inner region are matched with the asymptotic solutions (6) at the boundary $R = R_M$. Since the inner and outer solutions are expressed in two different coordinates, a simple frame transformation has to be made in matching.

The above procedures are carried out separately for both the initial states as well as the final states of different photon energies in the photoionization calculation. Once the initial- and final-state wave functions have been calculated the dipole transition matrix and thereby the photoionization cross sections of different photon energies can be obtained readily.

For both $(1s2s) \ ^1S^e$ and $(1s2s) \ ^3S^e$ initial states, 23 channels and 211 diabatic sectors with the matching distance $R_M = 22.8$ a.u. are used in the present calculation. The binding energies for $(1s2s) \ ^1S^e$ and $(1s2s) \ ^3S^e$ obtained are $-2.145\,980$ a.u. and $-2.175\,268$ a.u., to be compared with the experimental values $-2.146\,074$ a.u. and $-2.175\,330$ a.u. [7], respectively. For both $^1P^o$ and $^3P^o$ final-state wave functions, 25 channels and 341 diabatic sectors with $R_M = 99.5$ a.u. are used. Photoionization cross sections in both the dipole length and dipole acceleration forms are calculated. The two forms deviate from each other by less than 1% in the total cross section so they are indistinguishable in figures. For simplicity, the photoionization cross sections shown here are all in the dipole length form.

III. RESULTS AND DISCUSSIONS

A. He $(1s2s) \ ^1S^e \rightarrow \ ^1P^o$ photoionization

In terms of the approximate quantum numbers K, T, A and N, n [8], the doubly excited states associated with

the $N = 3$ manifold of $^1P^o$ symmetry are classified into five series: two of them belong to the $A = +$ series, ${}_N(K, T)_n^A = {}_3(1, 1)_n^+$, ${}_3(-1, 1)_n^+$ ($n = 3, 4, \dots$), two of them belong to the $A = -$ series, ${}_3(2, 0)_n^-$, ${}_3(0, 0)_n^-$, and one $A = 0$ series, ${}_3(-2, 0)_n^0$ ($n = 4, 5, \dots$). Generally, doubly excited states associated with $A = +$ series have larger widths, while the states with $A = -$ have smaller widths and the states with $A = 0$ have the smallest widths. For these states, there exist four dissociation channels: $1sep$, $2sep$, $2pes$, and $2ped$.

1. Total photoionization cross section

(i) *The calculated spectra.* Figure 1 shows the calculated total cross sections, plotted against the total energy E , of photoionization from the metastable $(1s2s)^1S^e$ state as well as from the ground state $(1s^2)^1S^e$ of He between the He^+ ($N = 2$) and ($N = 3$) thresholds. The resonances of different doubly excited states, all of them associated with the $N = 3$ manifold of $^1P^o$ symmetry, are labeled with the simplified notation K_n^A . In the photoionization from the ground state [Fig. 1(a)], it is evident that members of the 1_n^+ series are predominantly populated, while the $(-1)_3^+$ state, the first member of the second $+$ series, can also be observed as a small window-type resonance. But in the photoionization from the metastable $(1s2s)^1S^e$ state [Fig. 1(b)], the spectra are much richer and one sees that not only the 1_n^+ series but other series, such as $(-1)_n^+$ and 2_n^- series, are also very significant.

(ii) *The convoluted spectra.* The spectra in Fig. 1, where one assumes an infinite energy resolution, do not

allow us to easily see the spectral intensity of narrow resonances. To show which states have significant spectral intensity, it is more convenient to display the spectra obtained by convoluting the calculated spectra with the Gaussian distribution of a finite energy resolution. Of course, such convoluted spectra can then be directly compared with the experimental cross sections measured with that particular energy resolution. In Fig. 2, we show the spectra of Fig. 1 convoluted with a fictitious experimental energy resolution of 0.0002 a.u. or 5.4 meV, which is about the best resolution achievable nowadays [9]. (Denser energy points have been calculated near narrow $A = -$ and 0 states to ensure that their resonance profiles have been well resolved.) As expected, in Fig. 2 those sharp needle-like resonances in the calculated spectra (Fig. 1) have been suppressed according to their oscillator strengths while the broad resonances are almost unchanged by the convolution. In Fig. 2(a) the states belonging to the 1_n^+ series, the $+$ series with the maximum quantum number $K (= N - 2)$, is the only series primarily populated in photoionization from the ground state He, in accord with the propensity rule. This spectrum can be directly compared with the experimental spectrum of Domke *et al.* [9] which has an energy resolution of about 5 meV. For photoionization from the metastable state $(1s2s)^1S^e$ [Fig. 2(b)], the 1_n^+ series is still the most prominent one. However, $(-1)_3^+$, the first resonance state belonging to the $(-1)_n^+$ series, is also very significantly populated. The higher members of this series, which are very close to the neighboring 1_{n+1}^+ states, appear to have strong spectral intensities too as one can see from heights of their combined resonance peaks [for example, the peak formed by the $(-1)_4^+$ and 1_5^+ resonances is higher than

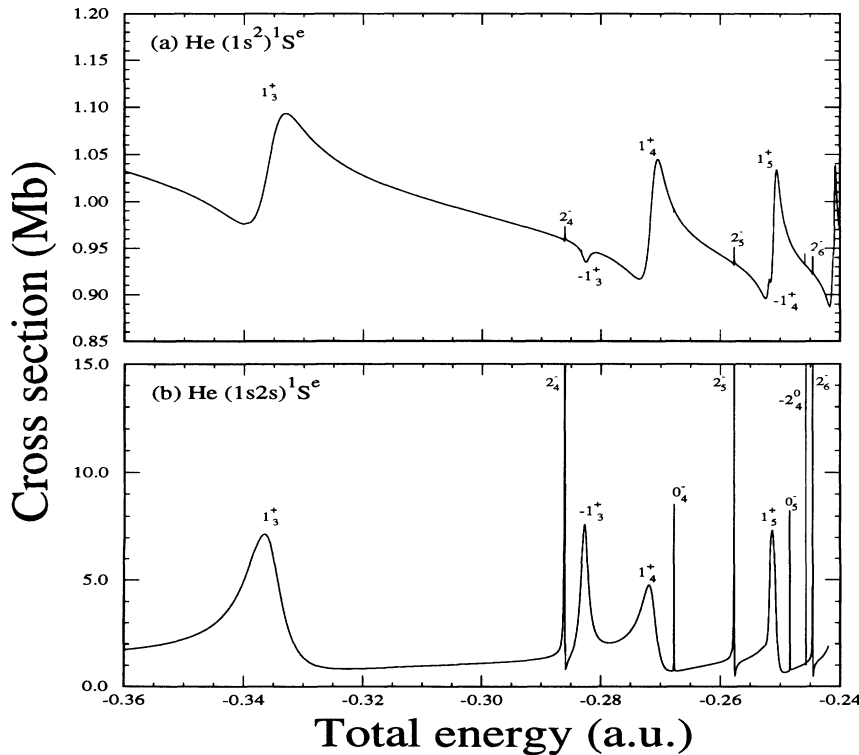


FIG. 1. The calculated total photoionization cross sections of He as functions of the total energy between the He^+ ($N = 2$) and ($N = 3$) thresholds: (a) from the ground state $(1s^2)^1S^e$, (b) from the $(1s2s)^1S^e$ state. The autoionizing doubly excited states are denoted with K_n^A .

the 1_4^+ peak]. Moreover, as is clearly seen from Fig. 2(b), the states of 2_n^- series are well populated. The other $A = -$ series, 0_n^- , is only weakly populated but still observable with 5.4 meV resolution. The $A = 0$ series (with much narrower widths) is even weaker and cannot be clearly resolved in this spectra. So similar to what has been found for the lower energies (below the $N = 2$ threshold) [1], Fig. 2 demonstrates that photoionization from the metastable state can provide a unique way to study doubly excited states, such as the 2_n^- series, which could not be easily observed in the photoionization from the ground state.

(iii) *The resonance parameters of the 1_3^+ state.* The resonance profiles of the first and most prominent state 1_3^+ in the calculated spectra from both the ground state and the metastable $(1s2s) 1S^e$ state have been fitted with the Fano formula

$$\sigma_{\text{tot}}(E) = \sigma_0 \left[\rho^2 \frac{(q + \varepsilon)^2}{1 + \varepsilon^2} + 1 - \rho^2 \right], \quad (7)$$

where $\varepsilon = 2(E - E_r)/\Gamma$, with E_r and Γ being the energy position and the autoionization width of the doubly excited state. The parameters $E_r, \Gamma, \sigma_0, \rho^2$, and q obtained from fitting the calculated spectra near the 1_3^+ resonance are tabulated in Table I. We see that the parameters obtained in the present calculation are in fair agreement with those of Sánchez and Martin [3], which are also listed in Table I. Although the background cross section σ_0 increases only slightly (note that the value of σ_0 obtained in the present work is larger than that of Sánchez and Martin [3]), the Fano shape parameter

TABLE I. Fano parameters of the He $3(1,1)_3^+ 1P^o$ resonance, for photoionization cross sections from the ground state $(1s^2) 1S^e$ and from the metastable $(1s2s) 1S^e$ state. The upper rows are present results and the lower rows are results from Sánchez and Martin [3].

	E_r (a.u.)	Γ (eV)	q	σ_0 (Mb)	ρ^2
$(1s^2) 1S^e$	0.3355	0.1893	1.26	1.030	0.0421
		0.1743	1.300	1.0007	0.0503
$(1s2s) 1S^e$			-3.97	1.2034	0.3226
			-4.610	0.9291	0.2974

q and the correlation coefficient ρ^2 for the spectra from the metastable state have changed drastically from those from the ground state, with q changing from 1.26 to -3.97 and ρ^2 from 0.0421 to 0.3226. These changes in both q and ρ^2 are expected from Figs. 1 and 2, where in the spectrum from the metastable state [Figs. 1(b), 2(b)] the 1_3^+ resonance is much stronger than the background and thus more Lorentzian shaped, compared with that in the spectrum from the ground state [Figs. 1(a), 2(a)]. The enhancement of ρ^2 , which is a measure of the overlap between the continuum populated by the direct dipole transitions and that populated by autoionizations of the doubly excited state, can be understood: The direct dipole transitions from the ground state populate primarily the $1sep$ channel while those from the metastable state populate primarily the $2sep$ channel, but in both cases the $N = 2$ continuum channels are the dominant autoionization channels, thus resulting in a larger ρ^2 for photoionization from the metastable state.

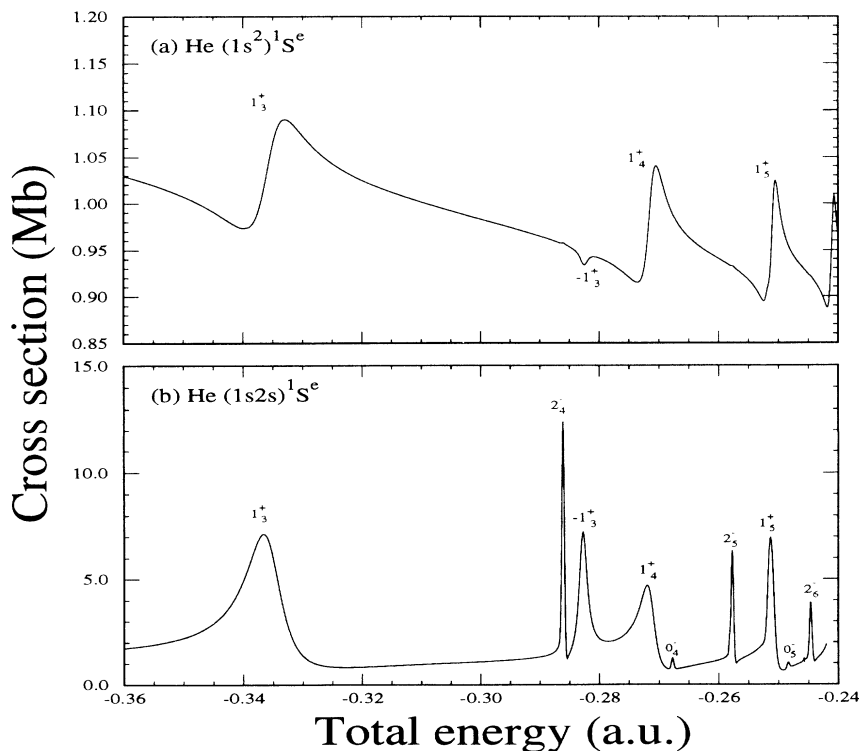


FIG. 2. The convoluted total photoionization spectra with the energy resolution 0.0002 a.u. of He: (a) from the ground state $(1s^2) 1S^e$, (b) from the $(1s2s) 1S^e$ state. The autoionizing doubly excited states are denoted with K_n^A .

2. Partial cross sections

The calculated partial photoionization cross sections from the metastable state $(1s2s)^1S^e$ to the $1s\epsilon p$, $2s\epsilon p$, $2p\epsilon s$, and $2p\epsilon d$ outgoing channels are displayed in Fig. 3. Note that the vertical scale of Fig. 3(a) for $\sigma_{1s\epsilon p}$ is ten times smaller, therefore the partial cross section to this channel is about ten times smaller than those to the $N = 2$ channels. One observes that the resonance structures in each channel are all very rich, as in the total cross section.

To make a more quantitative study, all partial cross

sections in the neighborhood of 1_3^+ resonance in Fig. 3 have been fitted with the following formula given by Starace [10]:

$$\sigma_j(E) = \frac{\sigma_0^j}{1 + \varepsilon^2} \{ \varepsilon^2 + 2\varepsilon[q\text{Re}(\alpha_j) - \text{Im}(\alpha_j)] + 1 - 2q\text{Im}(\alpha_j) - 2\text{Re}(\alpha_j) + (q^2 + 1)|\alpha_j|^2 \}. \quad (8)$$

The obtained partial background cross section σ_0^j and the complex parameters α_j for each channel j are tabulated and compared with their counterparts from the ground

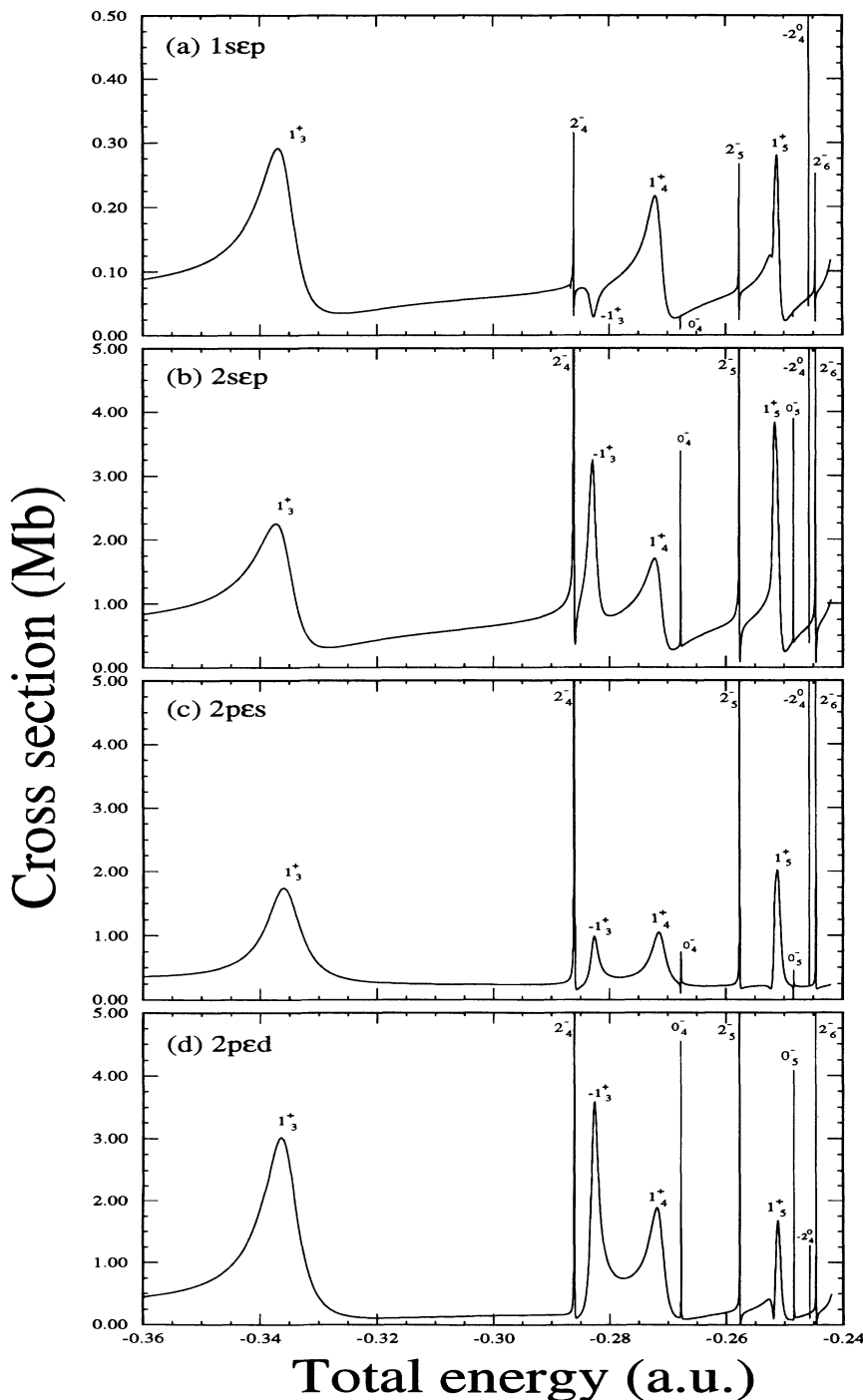


FIG. 3. The calculated partial cross sections of photoionization from the metastable $(1s2s)^1S^e$ state of He: (a) $\sigma_{1s\epsilon p}$; (b) $\sigma_{2s\epsilon p}$; (c) $\sigma_{2p\epsilon s}$; (d) $\sigma_{2p\epsilon d}$.

TABLE II. Resonance parameters and branching ratios for partial cross sections near the $1P^o$ $3(1,1)_3^+$ resonance of He. The upper rows are results for photoionization from the ground state and the lower ones are from the metastable state $(1s2s) 1S^e$.

j	σ_0^j (Mb)	$\text{Re}(\alpha_j)$	$\text{Im}(\alpha_j)$	$ \alpha_j ^2$	$100(\Gamma_j/\Gamma)^a$	$100(\Gamma_j/\Gamma)^b$
$1sep$	0.9313	-1.627×10^{-2}	-2.677×10^{-2}	9.814×10^{-4}	2.11	1.94
	0.0616	0.2728	0.2235	0.1244	1.97	2.01
$2sep$	0.0316	0.398	0.227	0.210	15.31	14.06
	0.6258	0.2557	0.1470	8.697×10^{-2}	14.70	15.03
$2pes$	0.0472	0.706	0.172	0.528	57.35	52.66
	0.2739	0.3477	-0.7789	0.7275	51.31	52.45
$2ped$	0.0232	0.666	0.442	0.639	34.16	31.37
	0.2301	0.5100	0.5049	0.5148	30.51	31.19

^aWithout the normalization, see text.

^bWith the normalization.

state in Table II. From these parameters, one can deduce the partial autoionization width Γ_j of channel j using a simple formula

$$\left(\frac{\Gamma_j}{\Gamma}\right) = \left(\frac{\sigma_0^j}{\sigma_0}\right) \left(\frac{|\alpha_j|^2}{\rho^2}\right). \quad (9)$$

The branching ratios Γ_j/Γ thus obtained are also listed in the table. The sums of the branching ratios $\sum_j(\Gamma_j/\Gamma)$ from the fitting are 1.089 and 0.978 for photoionizations from the ground and metastable states, respectively; both values are close to one, implying a good quality of the fitting. As shown in the last column of the table, the discrepancy between the two sets of branching ratios is significantly reduced when both are normalized so the sum is exactly one. This equality is expected since partial widths of the resonance are independent of the excitation mechanism.

Table II also gives the background partial cross sections near the 1_3^+ resonance, for photoionization from the ground state and the metastable $(1s2s) 1S^e$ state. From the ground state, the $1sep$ channel is the dominant continuum. From the metastable state, the transition to the $1sep$ channel is weak, but that to the $2sep$ channel is the

dominant one. This can be explained conveniently from an independent electron model where $1sep$ is the only allowed dipole transition channel from the ground state ($1s^2$) while $(1sep)$ and $(2sep)$ are the two allowed dipole transitions from the metastable state ($1s2s$). As the photon energies considered here are just slightly higher than the $2sep$ threshold but are much higher (more than ten times) than the $1sep$ threshold, the oscillator strength from the metastable state to the $2sep$ channel (equivalent to the single-electron transition $1s \rightarrow \epsilon p$) is much stronger than that to the $1sep$ channel (equivalent to the transition $2s \rightarrow \epsilon p$). However, the independent electron model fails to explain the significant population of the $2pes$ and $2ped$ channels, which can be understood only in terms of final-state electron-electron interactions if one starts from the independent electron approximation.

The values of $|\alpha_j|^2$ in Table II provide information about the fraction of the partial cross sections due to the autoionization of the doubly excited state. For photoionization from the ground state, σ_{1sep} is dominated by the direct dipole transition therefore $|\alpha_{1sep}|^2$ is only about 0.001. Conversely, for continuum channels associated with $N = 2$, the direct ionization to these channels is much weaker whereas the part due to the autoioniza-

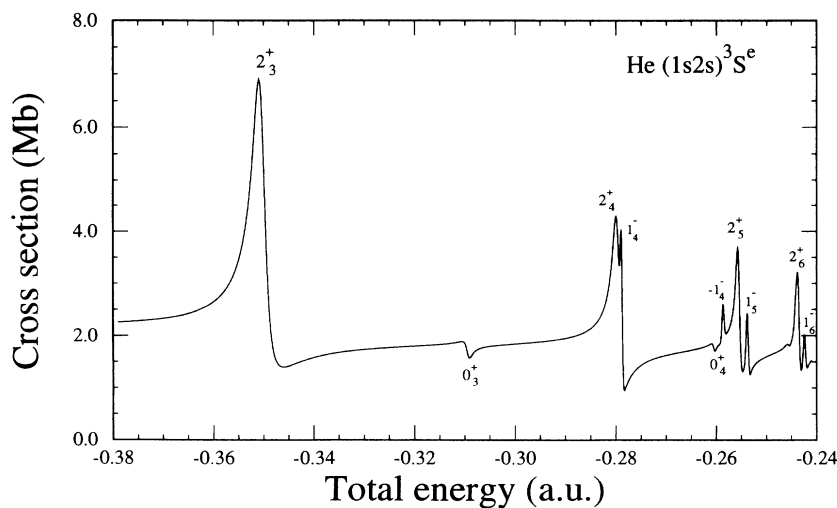


FIG. 4. Total photoionization spectrum from the metastable state $(1s2s) 3S^e$ of He convoluted with energy resolution 0.0002 a.u. The autoionizing doubly excited states are denoted with K_n^A .

tion of the doubly excited state accounts for more in the partial cross sections; as a result, the $|\alpha_j|^2$ values of the $N = 2$ channels are greatly larger than that of $|\alpha_{1sep}|^2$. For photoionization from the metastable state, the value of $|\alpha_{1sep}|^2$ is much larger than that from the ground-state ionization, due to the diminished direct ionization to the $(1sep)$ channel. By the same token, the value of $|\alpha_{2sep}|^2$ decreases from 0.210 of the ground-state ionization to

TABLE III. Fano parameters of the $\text{He } 3(2,0)_3^+ {}^3P^o$ resonance for photoionization cross sections from the metastable $(1s2s) {}^3S^e$ state. The upper rows are present results and the lower rows are results from Sánchez and Martín [4].

	E_r (a.u.)	Γ (eV)	q	σ_0 (Mb)	ρ^2
$(1s2s) {}^3S^e$	-0.3504	0.0820	-2.85	2.002	0.3028
	-0.350262	0.07703	-3.305	1.6136	0.2602

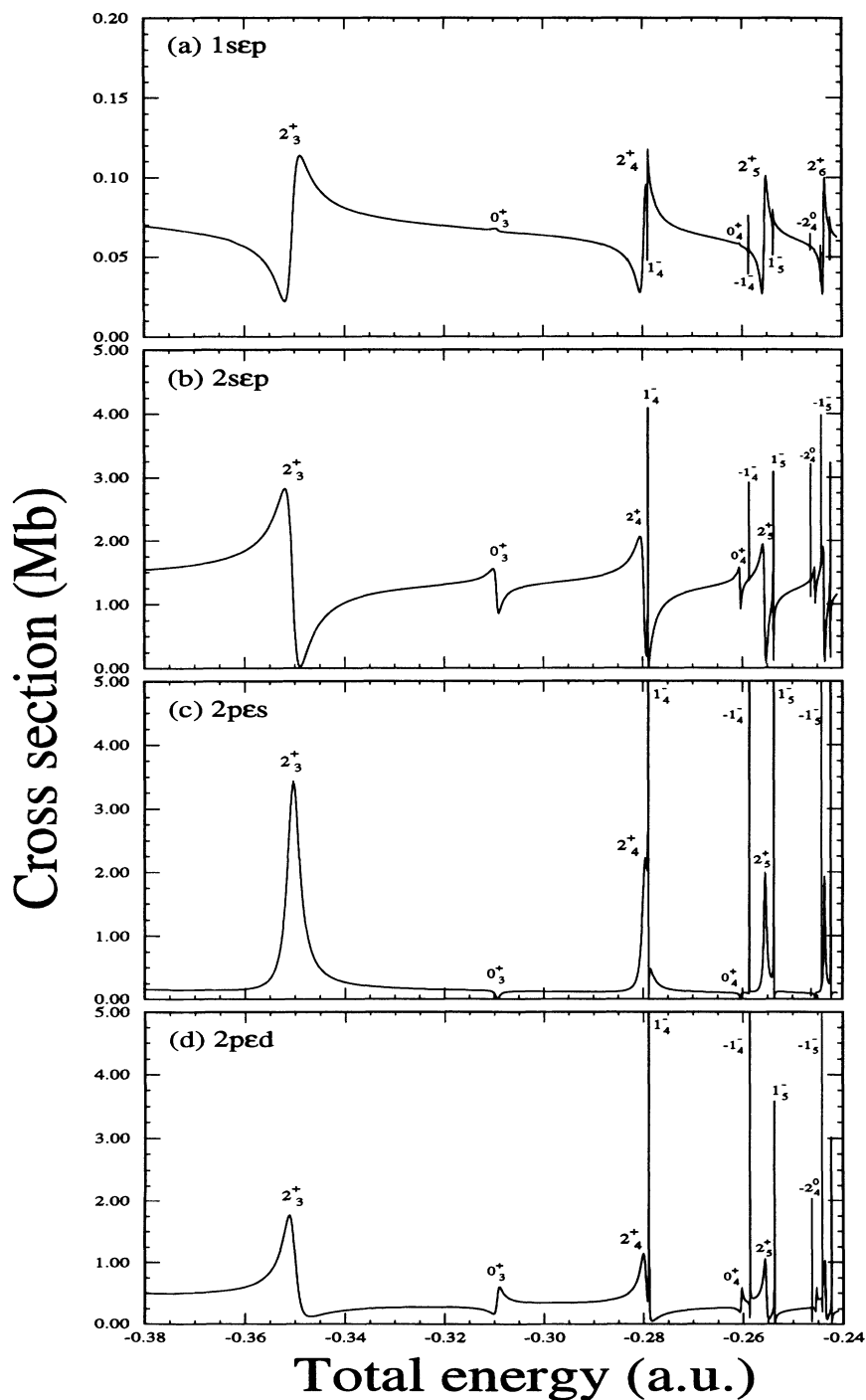


FIG. 5. The calculated partial cross sections of photoionization from the metastable state $(1s2s) {}^3S^e$ of He: (a) σ_{1sep} ; (b) σ_{2sep} ; (c) σ_{2pes} ; (d) σ_{2ped} .

0.087, thanks to a much enhanced direct transition to the $2s\epsilon p$ channel in photoionization from the metastable state.

B. He ($1s2s$) $^3S^e \rightarrow ^3P^o$ photoionization

We have also calculated the photoionization cross section of He from the metastable ($1s2s$) $^3S^e$ state. The five series of doubly excited states associated with the manifold $^3P^o(N=3)$ are two $A = +$ series, ${}_3(2,0)_n^+$, ${}_3(0,0)_n^+$, ($n = 3, 4, \dots$), two $A = -$ series, ${}_3(1,1)_n^-$, ${}_3(-1,1)_n^-$, and one $A = 0$ series, ${}_3(-2,0)_n^0$, ($n = 4, 5, \dots$). Note the approximate quantum numbers K, T of the $+$ and $-$ states of $^3P^o$ have been reversed from those of $^1P^o$ due to the total spin change.

1. Total photoionization cross section

The total photoionization cross sections obtained by convolution with an energy resolution of 0.0002 a.u. are shown in Fig. 4. From the figure, it is clear that the 2_n^+ series is the most prominent one while the 0_n^+ series is only weakly populated. In the meanwhile, both of the $A = -$ series, 1_n^- and $(-1)_n^-$, despite the narrowness in their autoionization widths, are significantly populated [the higher members of the $(-1)_n^-$ series are too close to the states of 2_n^+ series to be seen clearly]. The $A = 0$ series [its first member $(-2)_4^0$ is located between 1_5^- and 0_5^+] is too weak to be seen with the present resolution. The calculated total cross section near the neighborhood of the first resonance 2_3^+ has been fitted with the Fano formula (7) and the results are listed in Table III and are compared with the results obtained by Sánchez and Martin [4]. The two calculations are in reasonable agreement, but the cross sections from Sánchez and Martin [4] are somewhat lower. Notice that the q value is negative for this state.

2. Partial cross sections

In Fig. 5, the calculated partial cross sections are shown. Similar to the singlet state discussed above, the

partial cross sections of the $N = 2$ channels show more pronounced resonance structures than that of the $1\epsilon p$ channel, which is also significantly smaller in magnitude. It is also interesting to note that the shape of the autoionizing states depends so much on the particular continuum channel observed, as can be seen from Fig. 5.

The partial cross sections near the resonance 2_3^+ have been fitted with Eq. (8) and the results of σ_0^j , α_j , and the branching ratios Γ_j/Γ are tabulated and compared with those of Sánchez and Martin [4] in Table IV. The sum of the branch ratios obtained from the fitting is 1.0172; the branch ratios for the present work listed in the table have been normalized with the sum being equal to one. As expected from the independent electron model, from Table IV, the background for $\sigma_{2s\epsilon p}$ is the most dominant one and $\sigma_{1s\epsilon p}$ is almost negligible with respect to the total cross section. Analogous to the metastable singlet state photoionization, both σ_{2pes} and σ_{2ped} are significant. It is worthwhile to note, from Tables II and IV, that the $2s\epsilon p$ channel is more favored by the autoionization of the $^3P^o$ ${}_3(2,0)_3^+$ state than by the $^1P^o$ ${}_3(1,1)_3^+$ state. This difference partly causes the value of $|\alpha_{2s\epsilon p}|^2$ for the $^3P^o$ ${}_3(2,0)_3^+$ state to be much greater than that of the $^1P^o$ ${}_3(1,1)_3^+$ state populated from the metastable ($1s2s$) $^1S^e$ state.

IV. CONCLUSIONS

We have calculated photoionization cross sections of He from metastable states ($1s2s$) $^1S^e$ and ($1s2s$) $^3S^e$, for energies between the He⁺ ($N = 2$) and ($N = 3$) thresholds. The calculated spectra have been convoluted with an energy resolution of 5.4 meV so the spectral intensities of narrow states can be clearly seen. Contrary to photoionization from the ground state, where the $1\epsilon p$ is the dominant channel and only the $A = +$ series with the maximum K is populated, in photoionization from the metastable states the $N = 2$ channels make predominant contributions to the total cross section whereas the $1\epsilon p$ cross section is almost negligible. Furthermore, because the doubly excited states of the $N = 3$ manifold autoionize mostly via the $N = 2$ channels, the resonance structures in the $N = 2$ partial cross sections are much more pronounced than in the $\sigma_{1s\epsilon p}$. Consequently more series (including some narrow series with $A = -$) are sig-

TABLE IV. Comparison of resonance parameters and branching ratios for partial cross sections near the $^3P^o$ ${}_3(2,0)_3^+$ resonance of He. The upper rows are results from the present calculation and the lower ones are from Sánchez and Martin [4].

j	σ_0^j (Mb)	$\text{Re}(\alpha_j)$	$\text{Im}(\alpha_j)$	$ \alpha_j ^2$	$100(\Gamma_j/\Gamma)^a$
$1s\epsilon p$	0.0689	-0.1781	-0.1474	5.345×10^{-2}	0.5971
	0.0663	-0.1793	-0.1583	5.721×10^{-2}	0.9038
$2s\epsilon p$	1.4122	0.4008	-0.1526	0.1839	42.1084
	1.2657	0.3643	-0.0856	0.1400	42.2173
$2pes$	0.1403	-0.8574	1.0002	1.7355	39.4867
	0.0849	-1.3211	0.6384	2.1529	43.5155
$2ped$	0.3785	0.4856	0.2330	0.2901	17.8066
	0.1967	0.4210	0.3289	0.2854	13.3714

^a With the normalization, see text.

nificantly populated and become observable in the total photoionization cross sections from the metastable states. It is hoped that the calculations presented here will stimulate interest in experimental studies of photoionization from these metastable He states.

ACKNOWLEDGMENT

This work was supported in part by the U.S. Department of Energy, Office of Basic Energy Sciences, Division of Chemical Sciences.

-
- [1] B. Zhou, C.D. Lin, T.J. Tang, S. Watanabe, and M. Matsuzawa, *J. Phys. B* **26**, L337 (1993).
 - [2] R. Moccia and P. Spizzo, *J. Phys. B* **20**, 1423 (1987).
 - [3] I. Sánchez and F. Martin, *Phys. Rev. A* **47**, 1520 (1993).
 - [4] I. Sánchez and F. Martin, *Phys. Rev. A* **47**, 1878 (1993).
 - [5] J.Z. Tang, S. Watanabe, and M. Matsuzawa, *Phys. Rev. A* **46**, 2437 (1992).
 - [6] B. Zhou, C.D. Lin, J.Z. Tang, S. Watanabe, and M. Matsuzawa, *J. Phys. B* **26**, 2555 (1993).
 - [7] R.L. Kelly, Oak Ridge National Laboratory Report No. ORNL-5922, 1982 (unpublished). The conversion 1 a.u. (^4He)=27.207 696 eV is used.
 - [8] C.D. Lin, *Adv. At. Mol. Phys.* **22**, 77 (1986).
 - [9] M. Domke *et al.*, *Phys. Rev. Lett.* **66**, 1306 (1991).
 - [10] A.F. Starace, *Phys. Rev. A* **16**, 231 (1977).